Evaluating the impact of atmospheric CO2 emissions via super resolution of remote sensing data

Andrianirina Rakotoharisoa[1,2][0009−0005−2254−5911], Simone Cenci[3][0000−0001−6843−468X], and Rossella Arcucci[1,2][0000−0002−9471−0585]

[1] Department of Earth Science & Engineering, Imperial College London, London, SW7 2AZ, UK
[2] Data Science Institute, Imperial College London, London, SW7 2AZ, UK
[3] Imperial College Business School, London, SW7 2AZ, UK

Abstract. Understanding how emissions from point sources affect the atmospheric concentrations of Greenhouse Gases (GHGs) locally and on a wider scale is crucial to quantify their impact on climate change. To this end, different ways of performing global monitoring of GHGs concentration using remote sensing data have been explored. The main difficulty remains to find the right balance between high resolution monitoring, which is often incomplete, and global monitoring, but at a coarser resolution. This study proposes the application of Super Resolution (SR), a Deep Learning (DL) technique commonly employed in Computer Vision, to increase the resolution of atmospheric CO2 L3 satellite data. The resulting maps are achieving an approximate resolution of 1km*1km and are then compared with a benchmark of existing methods, before being used for emissions monitoring.

Keywords: Super Resolution · Remote Sensing · GHG Monitoring

1 Introduction and motivations

The latest Intergovernmental Panel on Climate Change (IPCC) report [4] asserts that GHGs, particularly CO_2 and CH_4, have contributed to the rise of the global surface temperature by over one degree since the late 19th century. Effective policies and measures to curb global warming are therefore conditioned by our understanding of GHG emissions. Remote sensing (RS) satellite imagery is used to generate estimations of concentration and can be improved for two reasons: it is either sparse following the satellite swath, or at a coarse resolution when processed. Machine learning approaches have helped to alleviate some of these data challenges. The present study concentrates on column-averaged dry air mole fraction of atmospheric CO2 (XCO2) monitoring and offers the following contributions:

- We generate SR maps of XCO2 with a spatial resolution of 0.03°*0.04°, 16-times higher than the original datasets from the Orbiting Carbon Obser-

ICCS Camera Ready Version 2024
To cite this paper please use the final published version:
DOI: 10.1007/978-3-031-63775-9_28

vatory 2 (OCO-2) Level 3 (L3) data. The model is not gas-specific and can therefore be adapted for monitoring other GHGs beyond CO2.
- We demonstrate that our model doesn't add noise to the original OCO-2 data and quantitatively improves compared to alternative methods.
- We propose an application of our dataset to the evaluation of CO_2 point sources' impact on their environment.

2 Related works

2.1 XCO2 modelling methods

Different forms of interpolations often following the model of Kriging have been implemented to build on sparse observations [8,22]. However, the quality of the generated products is variable following the density of the observations, leading to high uncertainty in some areas if no additional data is considered [14]. Data fusion approaches aim to reduce these uncertainties by combining data from multiple satellites [18]. Machine Learning (ML) and DL publications also often consider more variables as inputs [7]. For example, [11] combines XCO2 observations and environmental features such as meteorological and vegetation indicators before using Extra Randomised Trees. Chemical Transport Models (CTMs) generate simulations based on atmospheric dynamics and are good to predict fluxes [9,13]. It is however difficult to produce high resolution maps with these models due to their computational complexity.

2.2 Super Resolution

SR is a technique initially used in Computer Vision (CV) or image processing and aims to increase the resolution of an image by inferring high frequency details that were not available on the original image. It therefore creates a high resolution (HR) version of the input [15]. In the case of a single Low Resolution (LR) input, it is referred to as Single Image Super Resolution (SISR) [21]. If multiple LR inputs are used to generate the SR output, it becomes Multiple-Image SR.

3 Methods

3.1 Our model

In this study, input data consists of satellite-derived XCO2 L3 data (see Table 1). Transforming it from matrix form into RGB images requires additional data preprocessing steps and could potentially bias the SR output based on the colour scheme selection. Consequently, even though we approach the problem as a CV task, we treat the XCO2 maps as single-channel images and our model's design is a customized 1-channel implementation of the DL framework by Haris et al.[6] to deal with our data. The SR framework relies on iterative up- and down-sampling modules using convolutional and deconvolutional layers to learn the

ICCS Camera Ready Version 2024
To cite this paper please use the final published version:
DOI: 10.1007/978-3-031-63775-9_28

relationship between LR and HR pairs. To manage memory usage efficiently and improve training speed, we reconfigured the layers to minimize the number of parameters and utilized PyTorch's Distributed Data Parallel framework [12]. Originally designed to increase the resolution 8-fold, we adjusted the layers kernel size, padding, and stride for our purpose and have adapted the model for 16-fold upsampling, achieving an approximate resolution of 1km*1km, which is necessary for identifying individual emission sources.

Table 1: Data processing level definitions. Other levels are out of scope and therefore not included in this table.

Processing level definition	Definition
Level 2	Derived geophysical variables at the same resolution and location as Level 1 data
Level 3	Variables mapped on uniform space-time grids, usually with some completeness and consistency

4 Datasets

4.1 Training

Due to the absence of HR XCO2 data to train our model, the Land Surface Temperature (LST) dataset from MODIS [17] was used for training. We consider that temperature and XCO2, both being physical variables observed by satellites, exhibit similar variability as opposed to the natural images datasets typically used for training SR models. As shown in Table 2, LST data is first downsampled, using bicubic interpolation, before being reconstructed to its original resolution, which is in the same range as our target resolution for XCO2.

Table 2: Comparison of spatial resolution between data from OCO-2 and MODIS

	XCO2 L3 (OCO-2)	LST L3 (MODIS)
LR data (in degree)	0.5°*0.625°	0.8°*0.8°
HR data (in degree)	0.031°*0.039°(target)	0.05°*0.05°

ICCS Camera Ready Version 2024
To cite this paper please use the final published version:
DOI: 10.1007/978-3-031-63775-9_28

4.2 Low resolution and validation datasets

The OCO-2 and its successor OCO-3 are CO2 monitoring missions from NASA [5] with a radiometric resolution of the order of 1ppm. The L3 dataset generated from this mission [19] is used as our input data and consists of global maps of XCO2 at a resolution of 0.5°*0.625°. It is accessible at daily or monthly temporal granularity and is being generated through NASA's modeling and data assimilation framework.

The Total Column Carbon Network (TCCON) [20] is a network of fixed spectrometers located at various sites monitoring column concentrations from CO_2,CH_4, CO, and N_2O. We consider it as our groundtruth and compare the XCO2 values output by our model with the latest version of TCCON data [10]. The TCCON data was obtained from the TCCON Data Archive hosted by CaltechDATA at https://tccondata.org.

5 Results and Discussion

5.1 Benchmark

We benchmark our model against different approaches where the main criteria of selection were the temporal and spatial resolution of available data as well as metrics performance.

Table 3: Evaluation of our dataset against the benchmark

The best value for each metrics is in bolt. **LR** is the dataset from NASA, **BIC** is produced from bicubic interpolation, and **Fusion** is the fusion dataset [18]. The metrics are averaged over the TCCON network between 2015 and 2020

	SR (ours)	**LR**	**BIC**	**Fusion**
RMSE	**0.9180**	0.9441	0.9436	1.1196
R^2	**0.9673**	0.9654	0.9655	0.9514
MAE	**0.7027**	0.7182	0.7190	0.8505

The results in Table 3 show that our SR model is able to generate a HR version, enhanced 16-times, of the original dataset while improving on all metrics. This also holds true when comparing our maps with other methods. The fusion dataset has an average Root Mean Square Error (RMSE) of over 1ppm and a Mean Absolute Error (MAE) of 0.85ppm. These values are 20% higher relatively than the values of our model. Bicubic interpolation ranks second on most metrics. To further distinguish the performance of SR using our model versus using bicubic interpolation, we define an Improvement Ratio (IR) as follows:

$$IR^{site} = \frac{N^{site}_{improved}}{N^{site}_{samples}} \tag{1}$$

ICCS Camera Ready Version 2024
To cite this paper please use the final published version:
DOI: 10.1007/978-3-031-63775-9_28

For each site, $N^{site}_{improved}$ represents the number of instances where SR reduces the error compared to the ground truth, while $N^{site}_{samples}$ denotes the total number of samples for that site. A ratio of 1 (or 100%) indicates that the model consistently produces better results, while a ratio of 0 demonstrates that using this specific SR model always produces worse estimations.

Fig. 1: IR comparison between our model (blue) and bicubic (green) with available ground sensors data. An orange circle indicates that the IR ratio is over 50% for ours.

Figure 1 shows how the two SR models performs across different locations based on the IR. On 19 sites out of 24, our model improves on the LR input more frequently than the bicubic SR, which reflects that our model is more consistent.

5.2 Application: Impact of emissions on atmospheric CO2

Finally, we combine the information provided by our SR maps with the emissions dataset from ClimateTrace [3]. This is a first attempt to visualise how XCO2 can be influenced by point sources using HR global XCO2 maps. The dataset from ClimateTrace that we used is an inventory of CO_2 emissions point sources for the year 2021.

On Figure 2, the additional high-frequency details observable on the SR maps reveal that the locations of point sources do not necessarily coincide with the highest concentration in CO_2 in the area. This underscores the impacts point sources can have not only on their direct surroundings but also on areas seemingly far away or isolated from human activity. Furthermore, the influence of land topography on XCO2 is clearly pronounced and particularly visible on the Venezuelan area. High altitude areas serve as a natural obstacle and seem to direct the flow of CO_2. We must also note that other factors such as urbanisation may also influence XCO2 and are not visualised in our analysis.

ICCS Camera Ready Version 2024
To cite this paper please use the final published version:
DOI: 10.1007/978-3-031-63775-9_28

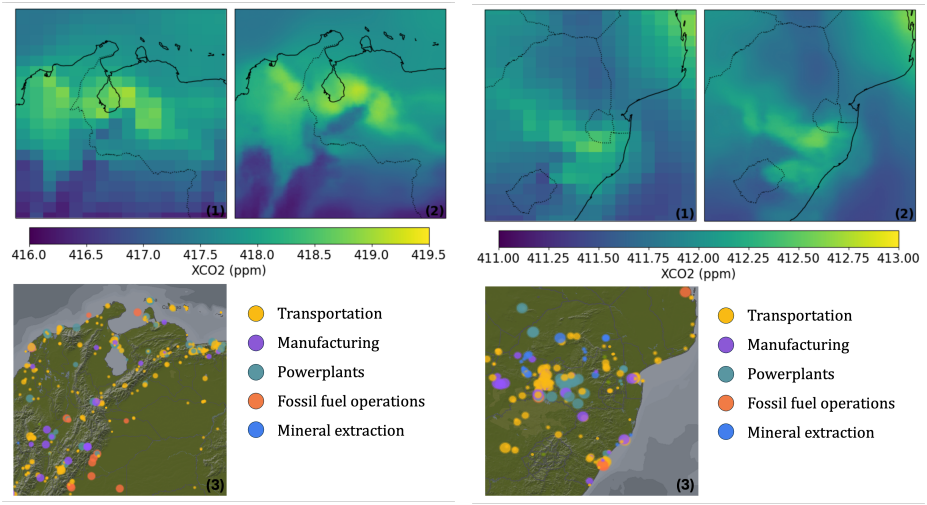

(a) Venezuela (b) South Africa

Fig. 2: Impact of point sources on XCO2 for the year 2021. For each subfigure from top left to bottom right: (1) is the LR map of the area studied, (2) is the super-resolved map, (3) is a map of CO_2 point sources extracted from the ClimateTrace emissions API.

5.3 Discussion

Based on the metrics selected for our benchmark, we showed that our model is better at estimating XCO2 while offering a higher resolution. However, we believe that we can improve its performance if we train the model on a physical variable closer to CO_2 than temperature. Furthermore, with existing Data Assimilation (DA) frameworks [2] and sparse satellite L2 data, our model could learn to further reduce misfits in speific areas. Another direction that could also be explored is the processing of multiple daily LR inputs to generate a single SR output, effectively reducing the temporal resolution of our dataset but also its uncerainty. Lastly, the application of SR maps in the context of point source monitoring needs to be expanded for a more comprehensive analysis.

6 Conclusion

This study has shown the potential of SR for upsampling the resolution of global L3 maps and generate HR XCO2 data. Although results are promising and improve on other methods listed in this paper, areas of improvement for our model have been identified and will be investigated in future works. We also proposed a visual analysis of CO_2 emission point sources and their impact on their environment, using the SR maps generated, which will be further explored. Finally, new XCH_4 L3 maps based on TROPOMI [16] should be released shortly [1]. The

ICCS Camera Ready Version 2024
To cite this paper please use the final published version:
DOI: 10.1007/978-3-031-63775-9_28

work presented in this study could therefore be applied to another GHG, which supports our implementation of a gas-agnostic framework.

Acronyms

CTM Chemical Transport Model
CV Computer Vision
DA Data Assimilation
DL Deep Learning
GHG Greenhouse Gas
HR high resolution
IR Improvement Ratio
LR Low Resolution
LST Land Surface Temperature
MAE Mean Absolute Error
ML Machine Learning
OCO-2 Orbiting Carbon Observatory 2
RMSE Root Mean Square Error
SISR Single Image Super Resolution
SR Super Resolution
TCCON Total Column Carbon Network
XCO2 column-averaged dry air mole fraction of atmospheric CO2

References

1. Balashov, N., Weir, B., Ott, L., Basu, S.: Generating global CH4 NASA GEOS product by assimilating TROPOMI. In: AGU Fall Meeting. No. A15L-1387 (2022)
2. Buizza, C., Quilodrán Casas, C., Nadler, P., Mack, J., Marrone, S., Titus, Z., Le Cornec, C., Heylen, E., Dur, T., Baca Ruiz, L., Heaney, C., Díaz Lopez, J.A., Kumar, K.S., Arcucci, R.: Data learning: Integrating data assimilation and machine learning. Journal of Computational Science **58**, 101525 (2022). https://doi.org/https://doi.org/10.1016/j.jocs.2021.101525, `https://www.sciencedirect.com/science/article/pii/S1877750321001861`
3. Climate TRACE coalition: Climate TRACE - Tracking Real-time Atmospheric Carbon Emissions. Climate TRACE Emissions Inventory (2022), `https://climatetrace.org/`
4. Core Writing Team, Lee, H., Romero, J.: Climate change 2023: synthesis report. Contribution of working groups I, II and III to the sixth assessment report of the intergovernmental panel on climate change pp. 35–115. https://doi.org/10.59327/IPCC/AR6-9789291691647
5. Eldering, A., Boland, S., Solish, B., Crisp, D., Kahn, P., Gunson, M.: High precision atmospheric CO2 measurements from space: The design and implementation of OCO-2. In: 2012 IEEE aerospace conference. pp. 1–10. IEEE (2012)
6. Haris, M., Shakhnarovich, G., Ukita, N.: Deep back-projectinetworks for single image super-resolution. IEEE Transactions on Pattern Analysis and Machine Intelligence **43**(12), 4323–4337 (2020)
7. He, C., Ji, M., Grieneisen, M.L., Zhan, Y.: A review of datasets and methods for deriving spatiotemporal distributions of atmospheric co2. Journal of Environmental Management **322**, 116101 (2022)

ICCS Camera Ready Version 2024
To cite this paper please use the final published version:
DOI: 10.1007/978-3-031-63775-9_28

8. He, Z., Lei, L., Zhang, Y., Sheng, M., Wu, C., Li, L., Zeng, Z.C., Welp, L.R.: Spatio-temporal mapping of multi-satellite observed column atmospheric co2 using precision-weighted kriging method. Remote Sensing **12**(3), 576 (2020)
9. Jacobson, A.R., Schuldt, K.N., Tans, P.: Carbontracker ct2022. NOAA Global Monitoring Laboratory (2023), https://doi.org/10.25925/Z1GJ-3254
10. Laughner, J.L., Toon, G.C., Mendonca, J., Petri, C., Roche, S., Wunch, D., Blavier, J.F., Griffith, D.W., Heikkinen, P., Keeling, R.F., et al.: The total carbon column observing network's ggg2020 data version. Earth System Science Data Discussions **2023**, 1–86 (2023)
11. Li, J., Jia, K., Wei, X., Xia, M., Chen, Z., Yao, Y., Zhang, X., Jiang, H., Yuan, B., Tao, G., et al.: High-spatiotemporal resolution mapping of spatiotemporally continuous atmospheric co2 concentrations over the global continent. International Journal of Applied Earth Observation and Geoinformation **108**, 102743 (2022)
12. Li, S., Zhao, Y., Varma, R., Salpekar, O., Noordhuis, P., Li, T., Paszke, A., Smith, J., Vaughan, B., Damania, P., et al.: Pytorch distributed: Experiences on accelerating data parallel training. arXiv preprint arXiv:2006.15704 (2020)
13. Pillai, D., Neininger, B.: Comparing lagrangian and eulerian models for co 2 transport–a step towards bayesian inverse modeling using wrf/stilt-vprm. Atmospheric Chemistry and Physics **12**(19), 8979–8991 (2012)
14. Sheng, M., Lei, L., Zeng, Z.C., Rao, W., Song, H., Wu, C.: Global land 1° mapping dataset of xco2 from satellite observations of gosat and oco-2 from 2009 to 2020. Big Earth Data **7**(1), 170–190 (2023)
15. Tsai, R.Y., Huang, T.S.: Multiframe image restoration and registration. Multiframe image restoration and registration **1**, 317–339 (1984)
16. Veefkind, J.P., Aben, I., McMullan, K., Förster, H., De Vries, J., Otter, G., Claas, J., Eskes, H., De Haan, J., Kleipool, Q., et al.: Tropomi on the esa sentinel-5 precursor: A gmes mission for global observations of the atmospheric composition for climate, air quality and ozone layer applications. Remote sensing of environment **120**, 70–83 (2012)
17. Wan, Z., Hook, S., Hulley, G.: Mod11c1 modis/terra land surface temperature/emissivity daily l3 global 0.05deg cmg v006 [data set] (2015), https://doi.org/10.5067/MODIS/MOD11C1.006
18. Wang, Y., Yuan, Q., Li, T., Yang, Y., Zhou, S., Zhang, L.: Seamless mapping of long-term (2010–2020) daily global xco 2 and xch 4 from the greenhouse gases observing satellite (gosat), orbiting carbon observatory 2 (oco-2), and cams global greenhouse gas reanalysis (cams-egg4) with a spatiotemporally self-supervised fusion method. Earth System Science Data **15**(8), 3597–3622 (2023)
19. Weir, B., Ott, L., OCO-2 Science Team: OCO-2 GEOS level 3 daily, 0.5x0.625 assimilated CO2 v10r (2021)
20. Wunch, D., Toon, G.C., Blavier, J.F.L., Washenfelder, R.A., Notholt, J., Connor, B.J., Griffith, D.W., Sherlock, V., Wennberg, P.O.: The total carbon column observing network. Philosophical Transactions of the Royal Society A: Mathematical, Physical and Engineering Sciences **369**(1943), 2087–2112 (2011)
21. Yang, W., Zhang, X., Tian, Y., Wang, W., Xue, J.H., Liao, Q.: Deep learning for single image super-resolution: A brief review. IEEE Transactions on Multimedia **21**(12), 3106–3121 (2019). https://doi.org/10.1109/TMM.2019.2919431
22. Zammit-Mangion, A., Cressie, N., Shumack, C.: On statistical approaches to generate level 3 products from satellite remote sensing retrievals. Remote Sensing **10**(1), 155 (2018)

ICCS Camera Ready Version 2024
To cite this paper please use the final published version:
DOI: 10.1007/978-3-031-63775-9_28